

Full Length Research Paper

Radiation effect on chemically reacting magnetohydrodynamics (MHD) boundary layer flow of heat and mass transfer through a porous vertical flat plate

S. Y. Ibrahim^{1*} and O. D. Makinde²

¹Department of Mechanical Engineering, Tamale Polytechnic, P. O. Box 3 E/R, Tamale, Ghana.

²Institute for Advance Research in Mathematical Modelling and Computations, Cape Peninsula University of Technology, South Africa.

Accepted 2 March, 2011

A mathematical model is presented for a two-dimensional, steady, viscous, incompressible, electrically conducting and laminar free convection boundary layer flow with radiation from a flat plate in a chemically reactive medium in the presence of a transverse magnetic field. The basic equations governing the flow are in the form of partial differential equations and have been reduced to a set of non-linear ordinary differential equations by applying suitable similarity transformations. The problem is tackled numerically using shooting techniques with the fourth order Runge-Kutta integration scheme. Pertinent results with respect to embedded parameters are displayed graphically for the velocity, temperature and concentration profiles and discussed quantitatively.

Key words: Heat transfer, thermal radiation, magnetic field, chemical species, mixed convection.

INTRODUCTION

Boundary layer flows induced over flat-plates by uniform free streams are well known in literature as Blasius (1908) problems. Howarth (1938) first conducted hand computations using Runge-Kutta numerical methods for flat plate flows. Thereafter, many authors investigated various aspect of the problem. Blasius solution for flow past a flat plate was investigated by Abussita (1994) and the existence of a solution was established. Asaithambi (1998) presented a finite-difference method for the solution of the Falkner-Skan equation and recently, Wang (2004) obtained an approximate solution for classical Blasius equation using Adomian decomposition method. Kuo (2004) studied the solutions of thermal boundary layer problems for flow past flat-plates using differential transformation method.

Convective heat transfer with thermal radiation is of

great importance in processes involving high temperatures such as in gas turbines, nuclear power plants, and thermal energy storage among others. Hossain and Takhar (1996) studied the effect of thermal radiation using the Rosseland diffusion approximation on mixed convection along a vertical plate with uniform free stream velocity and surface temperature. Similarly, Hossain et al. (1999a, 2001b) analysed the thermal radiation of a gray fluid which is emitting and absorbing radiation in a non-scattering medium. Later, Raptis et al. (2004) analysed the radiative flow in the presence of a magnetic field while Cortell (2007a, 2008b) studied the effects of thermal radiation on several distinct boundary layers. Cortell (2008a, 2008c) further studied radiation effects on Blasius and Sakiadis flows when plate is maintained at a constant temperature. He determined the effects of physical parameters like Prandtl number (Pr) and radiation parameter (N_R) on heat transfer characteristics. The free-convection flow with thermal radiation and mass transfer past a moving vertical porous

*Corresponding author. E-mail: yakubuseini@yahoo.com.

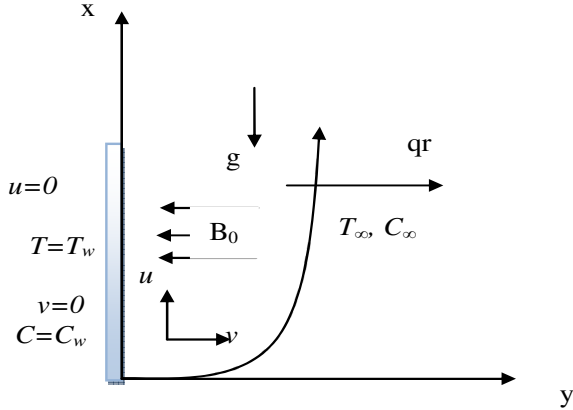


Figure 1. Physical configuration and coordinate system.

plate was investigated by Makinde (2005). Makinde et al. (2008) analysed the effect of thermal radiation on the heat and mass transfer flow of a variable viscosity fluid past a vertical porous plate permeated by a transverse magnetic field. The present study is an extension of Raptis et al. (2004) to include the combined effects of radiation and magnetic field strength in a chemically reactive medium as it has greater application in the industry.

PROBLEM FORMULATION

We consider a two-dimensional free convection effects on the steady incompressible laminar MHD heat and mass transfer characteristics of a radiated vertical plate, the velocity of the fluid far away from the plate surface is considered as the free stream value. The variations of surface temperature and concentration are linear. The flow configuration and coordinate system are shown in Figure 1.

All the fluid properties are assumed to be constant except for the density variations in the buoyancy force term of the linear momentum equation. The magnetic Reynolds number is assumed to be small, so that the induced magnetic field is neglected. No electrical field is assumed to exist and both viscous and magnetic dissipations are neglected. The Hall effects, the viscous dissipation and the joule heating terms are also neglected. Under these assumptions, along with Boussinesq approximations, the boundary layer equations describing the flow are summarized as follows;

$$\frac{\partial u}{\partial x} + \frac{\partial v}{\partial y} = 0, \quad (1)$$

$$u \frac{\partial u}{\partial x} + v \frac{\partial u}{\partial y} = \nu \frac{\partial^2 u}{\partial y^2} + g\beta_T(T-T_\infty) + g\beta_C(C-C_\infty) - \frac{\sigma_0^2}{\rho}(u-U_\infty), \quad (2)$$

$$u \frac{\partial T}{\partial x} + v \frac{\partial T}{\partial y} = \alpha \frac{\partial^2 T}{\partial y^2} - \frac{1}{\rho c_p} \frac{\partial q_r}{\partial y}, \quad (3)$$

$$u \frac{\partial C}{\partial x} + v \frac{\partial C}{\partial y} = D \frac{\partial^2 C}{\partial y^2}. \quad (4)$$

The appropriate boundary conditions for the problem are given as

$$u = v = 0, \quad T = T_w = T_\infty + ax, \quad C = C_w = C_\infty + bx, \quad \text{at } y = 0, \quad (5)$$

$$u = U_\infty, \quad T = T_\infty, \quad C = C_\infty, \quad \text{as } y \rightarrow \infty.$$

We use the Rosseland approximation for radiation of an optically thick boundary layer given by Raptis et al. (2004) and Cortel (2008b) in a simplified radiative heat flux form as

$$q_r = -\frac{4}{3} \frac{\sigma^*}{k^*} \frac{\partial T^4}{\partial y}, \quad (6)$$

where σ^* and k^* are the Stefan-Boltzmann constant and Rosseland mean absorption coefficient, respectively.

We assume that the temperature difference within the flow such as the term T^4 may be expressed as a linear function of temperature. Hence, expanding T^4 in a Taylor series about T_∞ (the fluid temperature at the free stream) and neglecting higher-order terms as in Bataller (2008), we obtain

$$T^4 \cong 4T_\infty^3 T - 3T_\infty^4. \quad (7)$$

Substituting Equations (6) and (7) into Equation (3) in the appropriate form leads to

$$u \frac{\partial T}{\partial x} + v \frac{\partial T}{\partial y} = \left(\alpha + \frac{16\sigma^* T_\infty^3}{3\rho c_p k^*} \right) \frac{\partial^2 T}{\partial y^2}, \quad (8)$$

where $\alpha = k / \rho c_p$ is the thermal diffusivity.

It is clear from Equation (8) that the effect of radiation is to enhance the thermal diffusivity. If we take, $N_R = \frac{kk^*}{4\sigma^* T_\infty^3}$ as the radiation parameter as in Bataller (2008), Equation (8) can be rewritten as

$$u \frac{\partial T}{\partial x} + v \frac{\partial T}{\partial y} = \frac{\alpha}{k_0} \frac{\partial^2 T}{\partial y^2}, \quad (9)$$

where

$$k_0 = \frac{3N_R}{3N_R + 4}. \quad (10)$$

We introduce the similarity variable η and the dimensionless

stream function $f(\eta)$ as

$$\eta = y \sqrt{\frac{U_\infty}{\nu x}} = \frac{y}{x} \sqrt{\text{Re}_x}, \quad f(\eta) = \frac{\psi(\eta)}{\sqrt{x \nu U_\infty}},$$

$$\theta(\eta) = \frac{T - T_\infty}{T_w - T_\infty}, \quad \phi(\eta) = \frac{C - C_\infty}{C_w - C_\infty}, \quad (11)$$

where $\theta(\eta)$ is a dimensionless temperature of the fluid in the boundary layer region, $\phi(\eta)$ is a dimensionless species concentration of the fluid, T represents temperature of the fluid and T_w is the temperature of the plate. T_∞ is the temperature of the fluid far away from the plate. Similarly, C represents the concentration of the chemical species in the fluid, C_w is the species concentration at the wall, C_∞ is the species concentration of the fluid far away from the plate. Thus, $T_w > T > T_\infty$ and $C_w > C > C_\infty$. With these set of dependent and independent variables, Equation (1) is satisfied simultaneously while Equations (2), (3), and (4) reduced to Equations (12), (13) and (14) respectively:

$$f''' + \frac{1}{2} f f'' + G_{Tx} \theta + G_{Cx} \phi - M(f' - 1) = 0, \quad (12)$$

$$\theta'' + \frac{\text{Pr} k_0}{2} f \theta' = 0, \quad (13)$$

$$\phi'' + \frac{Sc}{2} f \phi' = 0, \quad (14)$$

where primes denote differentiation with respect to η . The boundary conditions are also transformed into the following,

$$f' = 0, \quad f = 0, \quad \theta = 1, \quad \phi = 1, \quad \text{at } y = 0,$$

$$f' = 1, \quad \theta = 0, \quad \phi = 0, \quad \text{as } y \rightarrow \infty, \quad (15)$$

where

$$G_T = \frac{g \beta_T x (T_w - T_\infty)}{U_\infty^2}, \text{ is the local temperature Grashof}$$

$$\text{number, } G_C = \frac{g \beta_c x (C_w - C_\infty)}{U_\infty^2}, \text{ is the local concentration}$$

$$\text{Grashof number, and } M = \frac{\sigma B_0^2 x}{\rho U_\infty} \text{ is the local magnetic field}$$

NUMERICAL PROCEDURE

The set of Equations (11) to (14) under the boundary conditions (15) have been solved numerically using the Runge-Kutta parameter integration scheme with a modified version of the Newton-Raphson shooting method.

We let;

$$f = x_1, \quad f' = x_2, \quad f'' = x_3, \quad \theta = x_4, \quad \theta' = x_5, \quad \phi = x_6, \quad \phi' = x_7. \quad (16)$$

Equations (11) to (14) are transformed into systems of first order differential equations as follows;

$$x_1' = x_2,$$

$$x_2' = x_3,$$

$$x_3' = -\frac{1}{2} x_1 x_3 + M(x_2 - 1) - G_T x_4 - G_C x_6,$$

$$x_4' = x_5,$$

$$x_5' = -\frac{1}{2} \text{Pr} k_0 x_1 x_5,$$

$$x_6' = x_7,$$

$$x_7' = -\frac{1}{2} Sc x_1 x_7, \quad (17)$$

subject to the following initial conditions;

$$x_1(0) = 0, \quad x_2(0) = 0, \quad x_3(0) = s_1, \quad x_4(0) = 1,$$

$$x_5(0) = s_2, \quad x_6(0) = 1, \quad x_7(0) = s_3. \quad (18)$$

In a shooting method, the unspecified initial conditions; s_1, s_2 and s_3 in Equation (18) are assumed. Equation (17) is then integrated numerically as an initial valued problem to a given terminal point. The accuracy of the assumed missing initial condition is then checked by comparing the calculated value of the dependent variable at the terminal point with its given value there. If a difference exists, improved values of the missing initial conditions must be obtained and the process is repeated. The computations were done by a written program which uses a symbolic and computational computer language MAPLE. A step size of $\Delta \eta = 0.001$ was selected to be satisfactory for a convergence criterion of 10^{-7} in nearly all cases. The maximum value of η_∞ to each group of parameters Sc, M, G_T, G_C , and Pr is determined when the values of unknown boundary conditions at $\eta = 0$ not change to successful loop with error less than 10^{-7} . From the process of numerical computation, the local skin friction coefficient, the local Nusselt number and the local Sherwood number, which are respectively proportional to $f''(0), -\theta'(0)$, and $-\phi'(0)$ are worked out and their numerical values presented in Table 1.

RESULTS

Numerical results are reported in Table 1 and Figures 2 to 18. The Prandtl number was taken to be $Pr = 0.72$ which corresponds to air; the values of Schmidt number

Table 1. Computations showing $f''(0)$, $\theta'(0)$ and $\phi'(0)$ for various values of embedded parameter $Pr = 0.72$.

M	Sc	G_T	G_c	N_R	$f''(0)$	$-\theta'(0)$	$-\phi'(0)$
0.1	0.24	1	1	0.1	2.866119713808	0.161700863207	0.328152353412
0.5	0.24	1	1	0.1	2.715774578241	0.157411248176	0.314801374214
1.0	0.24	1	1	0.1	2.643497318099	0.153586285415	0.30305664137
0.1	0.62	1	1	0.1	2.695192292243	0.158655504441	0.483332708610
0.1	0.78	1	1	0.1	2.657009248999	0.158108875638	0.528123751194
0.1	2.64	1	1	0.1	2.475889567788	0.156053727069	0.825402340528
0.1	0.24	2	1	0.1	3.951783250461	0.174262325794	0.365670905056
0.1	0.24	3	1	0.1	4.956292787925	0.184369404514	0.394692607664
0.1	0.24	1	2	0.1	3.688807313223	0.167771186014	0.349825387426
0.1	0.24	1	3	0.1	4.452867338900	0.172780621291	0.367601468364
0.1	0.24	1	1	0.5	2.632252841126	0.281993102788	0.310074237495
0.1	0.24	1	1	1	2.546307639267	0.341497727175	0.303814500108
0.1	0.24	1	1	2	2.484472309332	0.392179538023	0.299598770273

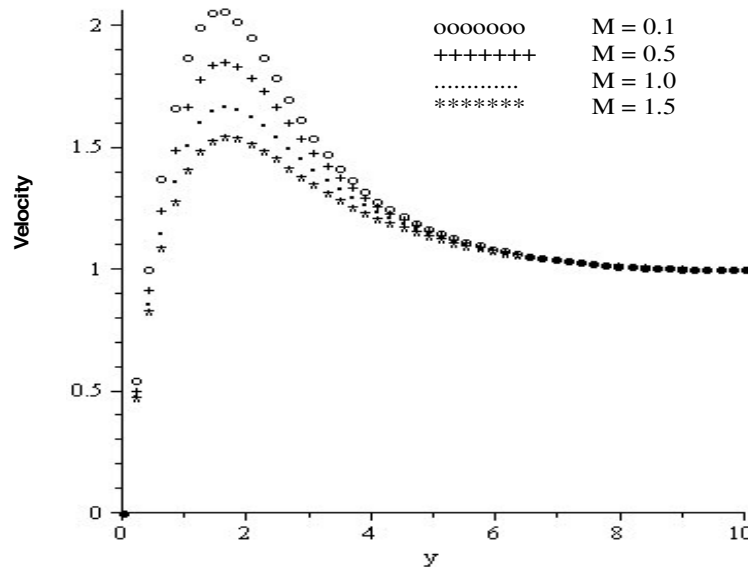


Figure 2. Velocity profile for $Pr = 0.71$, $Sc = 0.24$, $G_T = 1$, $G_c = 1$, $N_R = 0.1$.

(Sc) were chosen to be $Sc = 0.24, 0.62, 0.78, 2.62$, representing diffusing chemical species of most common interest in air like H_2, H_2O, NH_3 , and Propyl Benzene respectively. Attention is focused on positive values of the buoyancy parameters, that is, Grashof number $Gt > 0$ (which corresponds to the cooling problem) and solutal Grashof number $G_c > 0$ (which indicates that the chemical species concentration in the free stream region is less than the concentration at the boundary surface).

From Table 1, it is important to note that the skin

friction together with the heat and mass transfer rate at the plate surface decreases with increasing intensity of magnetic field (M). Also, the rate of heat and mass transfers at the plate surface increases with increasing intensity of buoyancy forces (G_T, G_c). Moreover, the skin friction and the surface heat transfer rate decreases, while the surface mass transfer rate increases with increasing Schmidt numbers. It is noted further that, increasing the radiation parameter (N_R) result in an increase in the heat transfer rate but a reduction in both

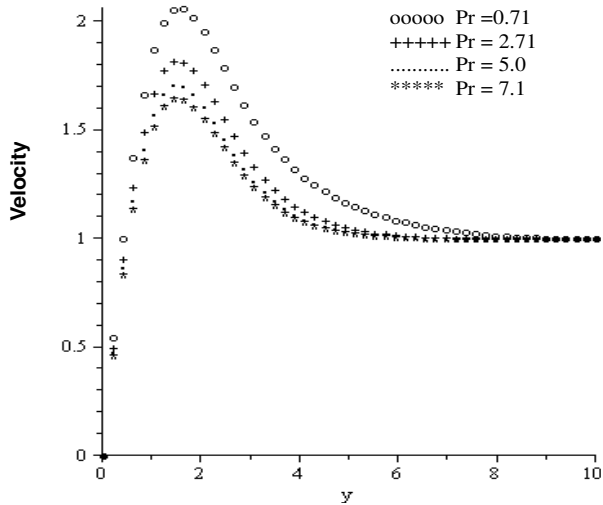


Figure 3. Velocity profile for $M = 0.1$, $Sc = 0.24$, $G_T = 1$, $G_c = 1$, $N_R = 0.1$.

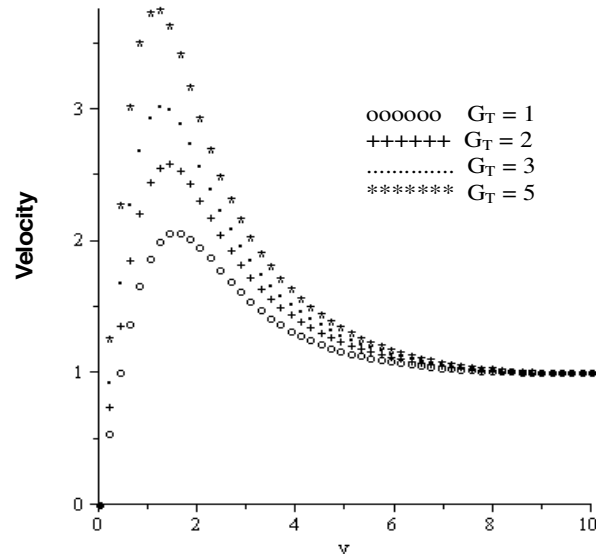


Figure 5. Velocity profile for $M = 0.1$, $Pr = 0.71$, $Sc = 0.24$, $G_c = 1$, $N_R = 0.1$.

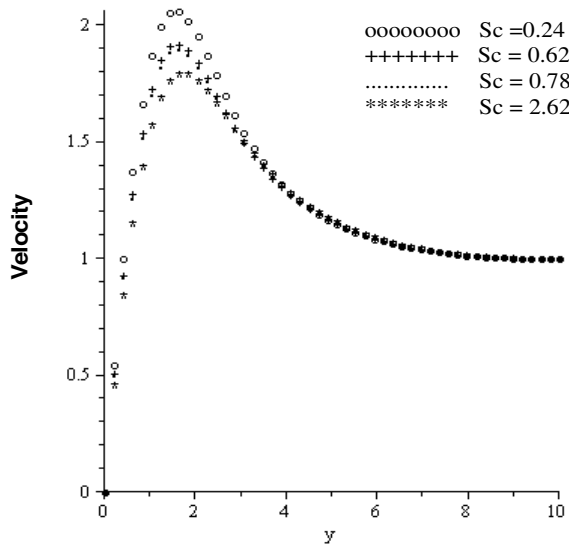


Figure 4. Velocity profile for $M = 0.1$, $Pr = 0.71$, $G_T = 1$, $G_c = 1$, $N_R = 0.1$.

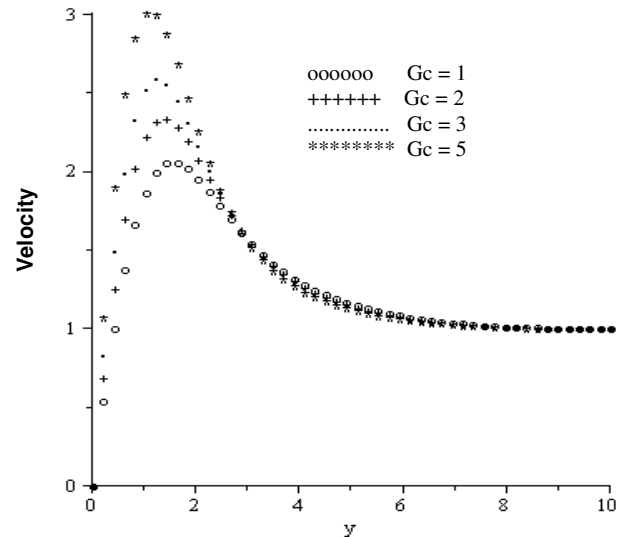


Figure 6. Velocity profile for $M = 0.1$, $Pr = 0.71$, $Sc = 0.24$, $G_T = 1$, $N_R = 0.1$.

the skin friction and the mass transfer rate.

DISCUSSION

Effect of parameter variation on velocity profiles

Figure 2 shows the effect of increasing the magnetic field strength on the momentum boundary-layer thickness. It is now a well established fact that increasing

the magnetic field strength dampened the velocity field by creating a drag force that opposes the fluid motion, causing the velocity to decrease. This force is known as the Lorentz force. Figures 3 and 4 show that when the Prandtl number or the Schmidt number increases, the velocity profile decreases. However, increasing the thermal and solutal Grashof parameters increases the velocity near the plate (Figure 5 and 6). This is as

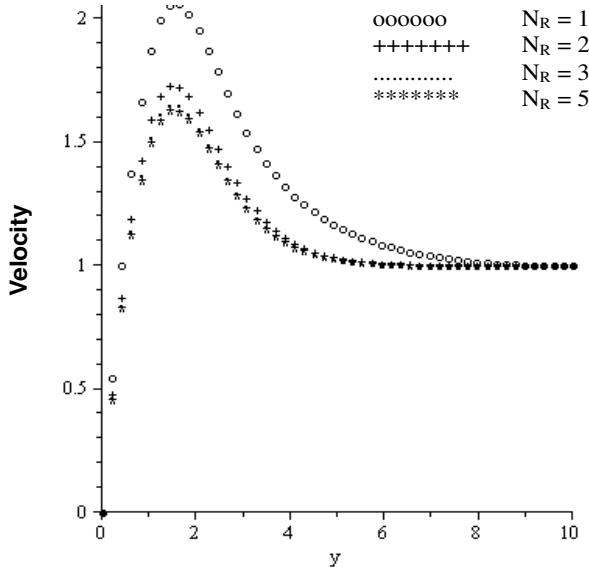


Figure 7. Velocity Profile for $M = 0.1$, $Pr = 0.71$, $Sc = 0.24$, $G_T = 1$, $G_c = 1$.

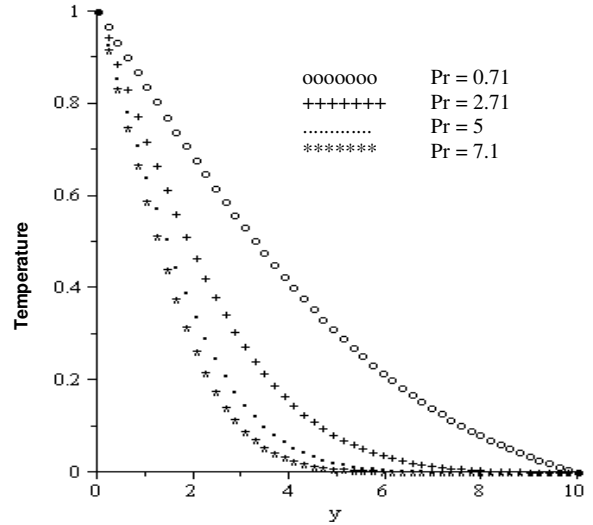


Figure 9. Dimensionless temperature profile when $M = 0.1$, $Sc = 0.24$, $G_T = 1$, $G_c = 1$, $N_R = 0.1$.

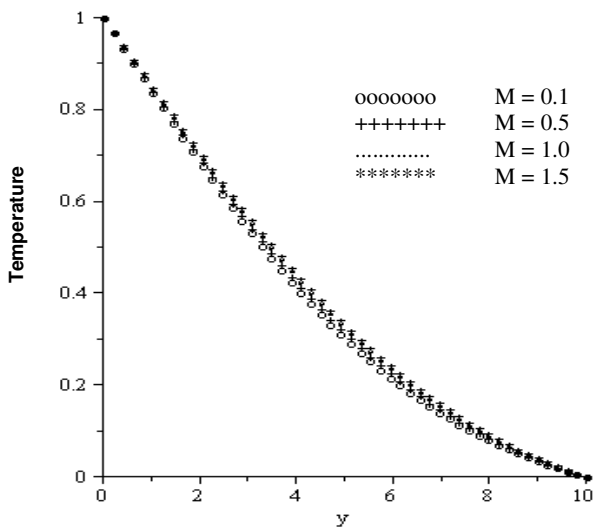


Figure 8. Temperature profile for $Pr = 0.71$, $Sc = 0.24$, $G_T = 1$, $G_c = 1$, $N_R = 0.1$.

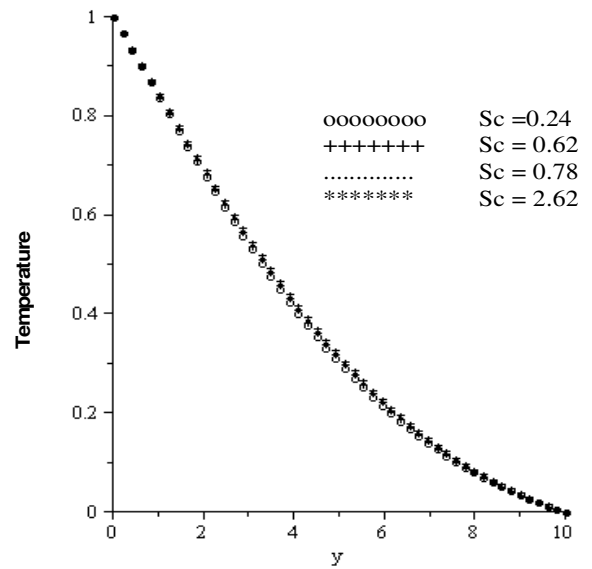


Figure 10. Temperature profile for $M = 0.1$, $Pr = 0.71$, $G_T = 1$, $G_c = 1$, $N_R = 0.1$.

expected because near a heat radiating plate, molecules of the fluid have higher activity due to the energy absorbed. Increasing the radiation parameter also reduces the velocity as illustrated in Figure 7. In all cases, the velocity at the plate surface is zero due to the 'no slip' condition. This increases to beyond the free stream value due to the radiated plate but settles down to the free stream value after some time.

Effects of parameter variation on temperature profiles

Figures 8 to 13 illustrate the effect of various parameter values on the thermal boundary layer thickness. In Figure 8, increasing the magnetic parameter results in a slight increase in the thermal boundary layer, whereas in Figure 9, there is a pronounced decrease in the thermal

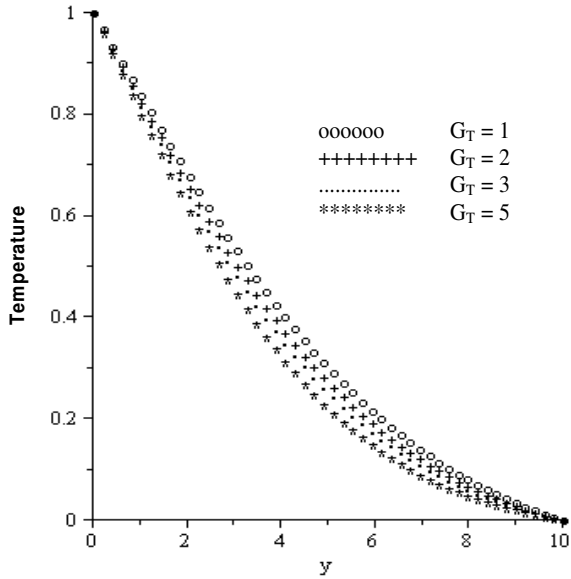


Figure 11. Temperature profile for $M = 0.1$, $Pr = 0.71$, $Sc = 0.24$, $G_c = 1$, $N_R = 0.1$.

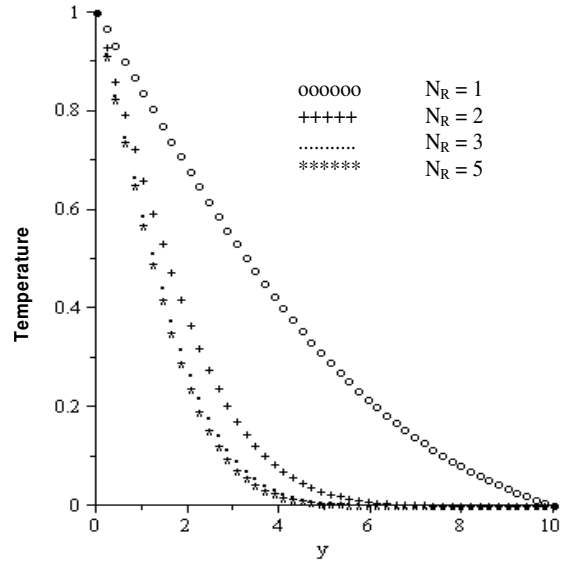


Figure 13. Temperature profile for $M = 0.1$, $Pr = 0.71$, $Sc = 0.24$, $G_T = 1$, $G_c = 1$.

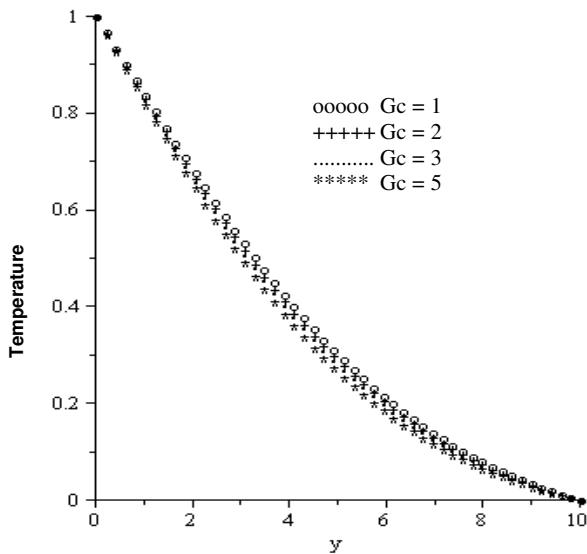


Figure 12. Temperature profile for $M = 0.1$, $Pr = 0.71$, $Sc = 0.24$, $G_T = 1$, $N_R = 0.1$.

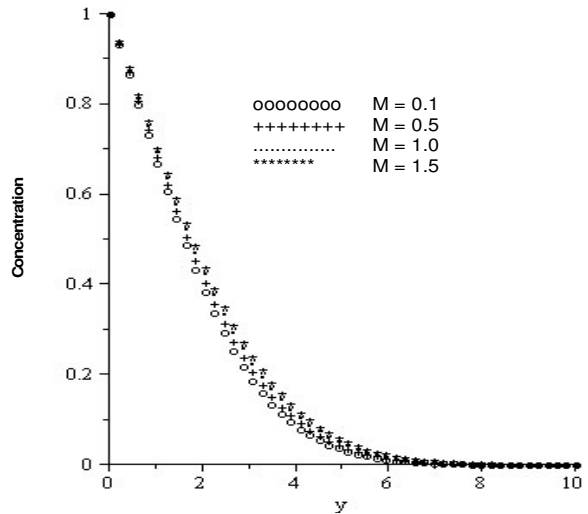


Figure 14. Concentration profile for $Pr = 0.71$, $Sc = 0.24$, $G_t = 1$, $G_c = 1$, $N_R = 0.1$.

boundary layer when the Prandtl number is increased. Increasing the Schmidt number as in Figure 10 results in a slight increase in the thermal boundary layer, however, increase in thermal and solutal Grashof numbers, as well as the radiation parameter (Figures 11 to 13) respectively, causes a reduction in the thermal boundary layer thickness.

Effects of parameter variation on concentration profiles

Figures 14 to 19 depict chemical species concentration profiles against spanwise coordinate η for varying physical parameter values in the boundary layer region. The species concentration is highest at the plate surface and decreases to zero far away from the plate satisfying the boundary condition. It is noted that the concentration

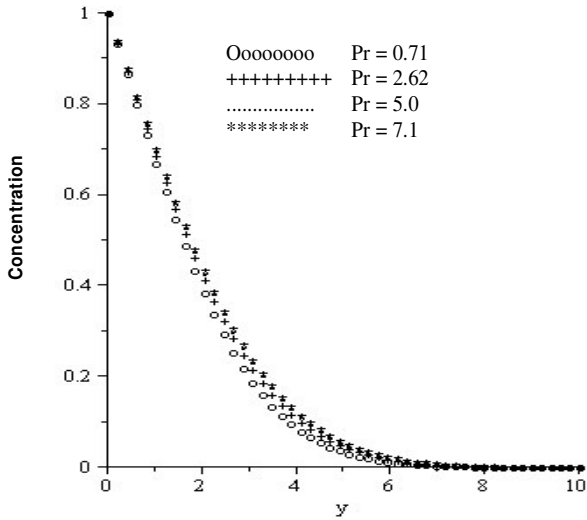


Figure 15. Dimensionless concentration profile when $M = 0.1$, $Sc = 0.24$, $G_T = 1$, $G_c = 1$, $N_R = 0.1$.

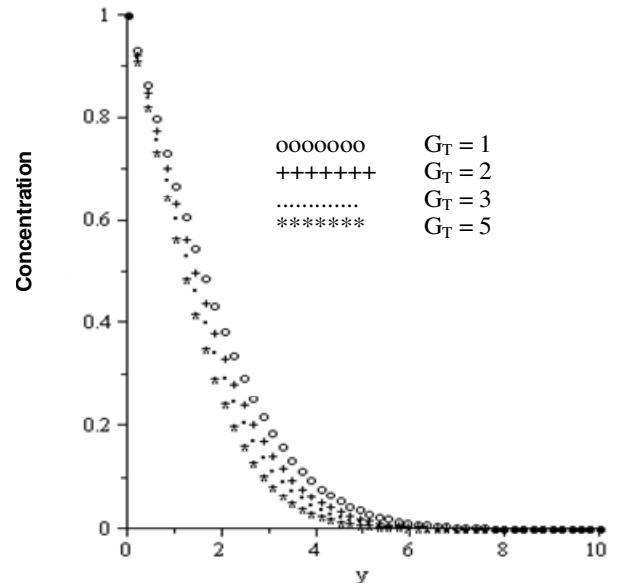


Figure 17. Concentration profile for $M = 0.1$, $Pr = 0.71$, $Sc = 0.24$, $G_c = 1$, $N_R = 0.1$.

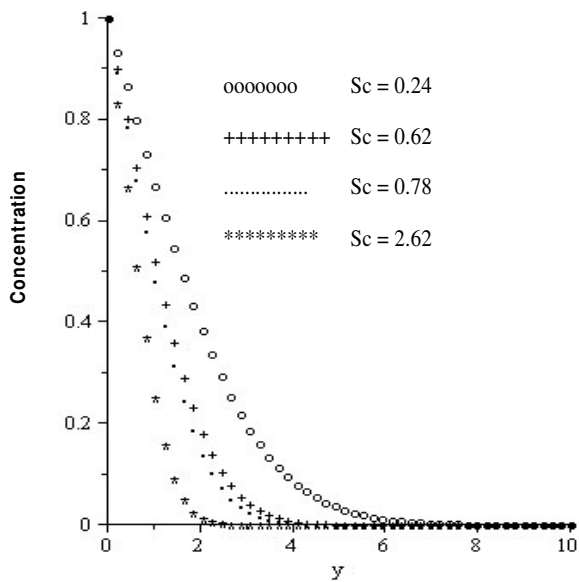


Figure 16. Concentration profile for $M = 0.1$, $Pr = 0.71$, $G_T = 1$, $G_c = 1$, $N_R = 0.1$.

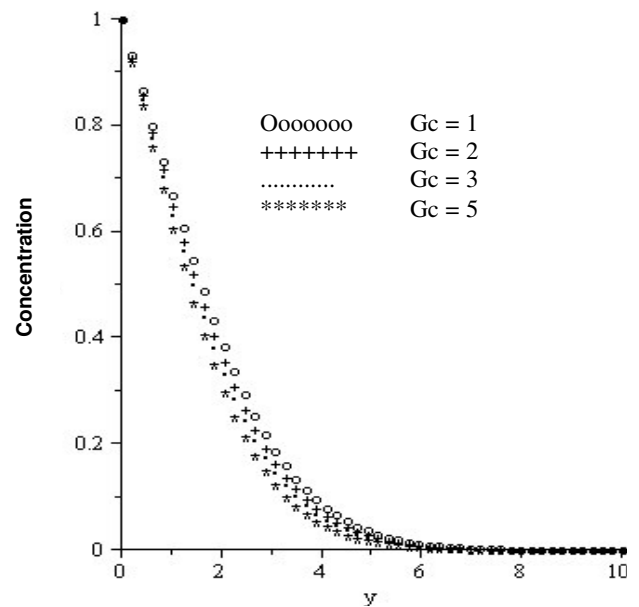


Figure 18. Concentration profile for $M = 0.1$, $Pr = 0.71$, $Sc = 0.24$, $G_T = 1$, $N_R = 0.1$.

boundary layer thickened with increasing values of the magnetic parameter and Prandtl numbers (Figures 14 and 15). It can be observed further that increasing the values of the Schmidt number, the thermal and solutal Grashof numbers reduce the concentration boundary layer (Figures 15 to 18). In Figure 18, the radiation parameter is observed to increase with the concentration boundary layer.

Conclusion

An IVP procedure is employed to give numerical solutions of the Blasius momentum boundary layers across a vertical flat-plate and heat transfer in the presence of thermal radiation under a convective surface

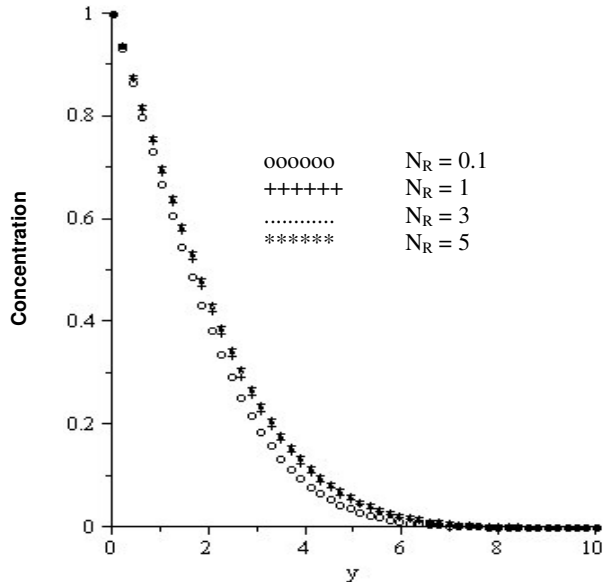


Figure 19. Concentration profile for $M = 0.1$ $Pr = 0.71$, $Sc = 0.24$, $G_T = 1$, $G_c = 1$.

boundary condition. The transformed partial differential equations together with the boundary conditions are solved numerically by a shooting 4th order Runge-Kutta procedure. The combined effect of increasing the Prandtl number and the radiation parameter tend to reduce the thermal boundary layer thickness along the plate. This yields a reduction in the fluid temperature. In general, the Blasius flow provides a thicker thermal boundary layer but this trend can be reversed at low values of parameters entering the problem.

REFERENCES

- Abussita AMM (1994). A note on a certain boundary-layer equation, *Appl. Math. Comp.*, 64: 73-77.
- Asaithambi A (1998). A finite-difference method for the Falkner–Skan equation, *Appl. Math. Comp.*, 92: 135-141.
- Bataller RC (2008). Radiation effects for the Blasius and Sakiadis flows with a convective surface boundary condition. *Appl. Math. Comput.*, 198: 333-338.
- Cortell R (2007a). Effects of heat source/sink, radiation and work done by deformation on flow and heat transfer of a viscoelastic fluid over a stretching sheet. *Comput. Math. Appl.* 53: 305-316.
- Cortell R (2008a). Similarity solutions for boundary layer flow and heat transfer of a FENE-P fluid with thermal radiation. *Phys. Lett. A.* 372: 2431-2439.
- Cortell R (2008b). Effects of viscous dissipation and radiation on the thermal boundary layer over a nonlinearly stretching sheet. *Phys. Lett. A.*, 372: 631-636.
- Cortell R (2008c). Radiation effects in the Blasius flow, *Appl. Math. Comp.*, 198: 333-338.
- Hossain MA, Alim MA, Rees D (1999a). The effect of radiation on free convection from a porous vertical plate. *Int. J. Heat Mass Transfer*, 42: 181-191.
- Hossain MA, Khanafar K, Vafai K (2001b). The effect of radiation on free convection flow of fluid with variable viscosity from a porous vertical plate. *Int. J. Therm. Sci.*, 40: 115-124.
- Howarth L (1938). On the solution of the laminar boundary layer equations, *Proc. Roy. Soc. of London*, 164: 547-579.
- Kuo BL (2004). Thermal boundary-layer problems in a semi-infinite flat plate by the differential transformation method, *Appl. Math. Comp.*, 150: 303-320.
- Makinde OD (2005). Free-convection flow with thermal radiation and mass transfer past a moving vertical porous plate. *Int. Comm. Heat Mass transfer*, 32: 1411-1419.
- Makinde OD, Ogulu A (2008). The Effect of Thermal Radiation on Heat and Mass Transfer Flow of a Variable Viscosity Fluid Past a Vertical Porous Plate Permeated by a Transverse Magnetic Field. *Chem. Eng. Comm.*, 195(12): 1575-1584.
- Raptis A, Perdikis C, Takhar HS (2004). Effect of thermal radiation on MHD flow, *Appl. Math. Comp.*, 153: 645-649.
- Wang L (2004). A new algorithm for solving classical Blasius equation, *Appl. Math. Comp.*, 157: 1-9.